Reverse horseshoe and spiral templates in an erbium-doped fiber laser

Javier Used and Juan Carlos Martín*
Department of Applied Physics, University of Zaragoza, C/Pedro Cerbuna, 12-E50009 Zaragoza, Spain
(Received 23 September 2008; revised manuscript received 30 January 2009; published 13 April 2009)

Time series obtained from the emission of an erbium-doped fiber ring laser with sine-wave pump modulation have been analyzed in order to determine the topological structure of the underlying chaotic attractor. With appropriate modulation conditions, topological structures not often observed in experimental systems have been found: the reverse horseshoe and the spiral template. The method employed for template determination is not conventional as it takes profit of the high dissipation of the system, which allows one to simplify dramatically the general procedure of analysis.

DOI: 10.1103/PhysRevE.79.046213 PACS number(s): 05.45.Ac, 05.45.Tp

I. INTRODUCTION

Since the moment that the concept of chaotic attractor was proposed, the problem of its characterization arose. Several parameters were suggested, some of them are widely used today such as Lyapunov exponents, fractal dimension, or entropies, which are useful to quantify the degree of complexity of the chaotic attractor. Nevertheless, the information provided by these parameters is reduced because they do not describe the attractor structure. In order to do so, an object suitable to characterize the attractor (the template) and a procedure to find this object have been proposed for systems whose dynamics can be modeled by a three-dimensional phase space or which rapidly relax to a three-dimensional subspace of the phase space. Both the object and the procedure are based on the Birman-Williams theorem [1,2] which shows that there is a one-to-one correspondence between the periodic orbits in flows in $R^2 \times S^1$ having a contracting direction and the orbits in a branched manifold which can be thought of as the "limit for infinite contracting rate" of the flow. Such a branched manifold is called "template" or "knot holder." In general, a template may be a very complex object (see [3] for a thorough template classification), but templates required to describe physical phenomena are much simpler, as explained in Sec. II. They can be fully characterized by means of integer numbers, which allow one to get a clear answer with regard to the validity of a theoretical model candidate to account for an experimental time series: if the analysis of the theoretical and the experimental time series provides different templates, the model is not valid, at least with the parameters chosen for the simulation (when dealing with real parameters, frequently the answer is not that clear: whether the model is valid or not depends on the tolerable difference between the theoretical and experimental values of the parameters chosen; in the end, tolerance is a subjective matter).

Concerning the procedure to find the template, it is based on a rather straightforward consequence of the Birman-Williams theorem [1,2,4]: the unstable periodic orbits (UPOs) in the flow present the same linking numbers than their projections in the template. The procedure allows determination of the template which rules the dynamics of a system departing from a time series. This technique has been described in several references (see, for instance, [5–7] and especially Appendix A of [8] for a detailed explanation). An interesting different procedure based on the study of the UPOs' braids can be found in [4,9]. Several authors have applied these topological analysis techniques to a number of dynamical systems [4–15].

We present the analysis of two time series extracted from the emission of an erbium-doped fiber ring laser. The interest of the results obtained is double. On the one hand, the system is highly dissipative (the laser cavity losses are around 85%). Due to this property, the Poincaré sections (PSs) obtained after a suitable embedding turn out to be thin enough to be considered as a line. This fact allows one to make use of methods of analysis habitually impossible to apply and simpler than usual. On the other hand, the templates which summarize the topological structure of the two corresponding attractors are found to be a reverse horseshoe and a spiral template. The interest of these structures is due to its exceptionality: in most of the previous studies on experimental systems, the template obtained is a Smale horseshoe, often with zero global torsion. Structures such as the reverse horseshoe or the spiral template have been very scarcely reported. Particularly, reports on the reverse horseshoe reduce to [13], while there are a few more reports on spiral templates: they can be found in [11,16–18]. Results different from the ubiquitous Smale horseshoe are attractive because they enforce the usefulness of topological analysis: obviously, a technique of analysis which would always provide the same final result would present no interest; it is the existence of a richer variety of possible solutions in nature which endows templates with practical relevance.

II. SUMMARY OF THE PROCEDURE OF ANALYSIS

We consider convenient to provide here a brief review of the topological analysis procedure. Its aim is the determination of the template which rules the dynamics of a given time series. In general, templates present several branches which stem from and converge to different trunks [3,11], but up to the moment templates with only one trunk have sufficed to model experimental time series, so we will restrict ourselves to them. These templates are fully characterized by pointing

*jcmartin@unizar.es

out their branches' torsions, the number of rotations of each branch around each one of the other branches, and the piling order of the branches when they converge to a single trunk. Besides, templates compatible with a physical phenomenon must satisfy a continuity condition: if we denote the action of the flow on a point x in phase space after a time t has passed as $\Phi_t(x)$, the following condition must be satisfied:

$$\lim_{\varepsilon \to 0}[\Phi_t(x+\varepsilon) - \Phi_t(x)] = 0. \quad (1)$$

This requirement implies several relations among the torsions of the different branches as well as among the number of turns of the different pairs of branches: for instance, the torsion of two consecutive branches must differ in one half-turn.

Once an embedding has been constructed from the experimental time series, the initial step of the procedure is the identification of UPOs in the time series under study. UPOs are identified by looking for close returns in a PS ("close returns" are intersections of the orbit with the PS whose distance is less than a suitable upper bound). Several techniques have been proposed [19–21]. The UPO period is easy to determine: if the close returns correspond to two consecutive intersections of the flow with the PS, it deals with a "period 1" orbit. In general, if $N-1$ intersections occur between the close returns found, the period of the orbit detected is N. Next, the linking numbers of each pair of UPOs as well as the self-linking number of each UPO must be computed. If a generating partition can be established prior to the analysis (for instance, if the system presents a one-to-one first-return map), the UPO symbolic names are clearly defined. For each linking number or self-linking number determined, an equation can be formulated which relates this linking number with the above-mentioned features necessary to characterize the template [8,15,22]: the piling order of the branches, their torsions, and the number of rotations of each branch around each one of the other branches. If enough linking numbers are available, it is possible to configure a system with sufficient equations to determine all the elements of the template and insertion matrices.

Nevertheless, usually no generating partition can be established beforehand. Therefore, neither the number of template branches nor the orbit name is known before the analysis. In this case, the way to proceed [8,15] consists of starting considering a template as simple as possible: with only two branches. All combinations of orbit names with two symbols must be tried. Some of them may give rise to an inconsistent system of equations or to a consistent system of equations whose algebraic solution (or solutions) corresponds to nonsense template parameters (for instance, noninteger number of half torsions of any branch or templates not compatible with the continuity requirement). In both cases, the corresponding combinations are ruled out. If no combinations giving rise to a valid template solution are found, one more branch is added to the template and the process is iterated until one or several solutions compatible with a certain combination of orbit names are found.

Application of the topological analysis procedure does not always lead to a right unique template. Of course, possibly the template obtained will be wrong if there are mistakes in UPO identification or in the computing of the linking numbers (certainly, both operations are not trivial, mainly in experimental signals which are unavoidably affected by noise). But even in case that all UPOs and linking numbers have been obtained correctly, sometimes there are problems in the identification of the template because there are not enough data. Two kinds of problems can be observed: either different possible solutions are found, because the linking numbers obtained are compatible with various combinations of UPO names, each one corresponding to a different template, or the procedure leads to wrong solutions—templates compatible with the set of linking numbers obtained with less number of branches than the template that really rules the system dynamics. Obviously, none of these problems appear in cases in which a one-to-one return map can be found: in these situations, both the number of branches in the template and the name of each UPO are clearly defined, and a few UPOs suffice to determine the template unambiguously.

III. ANALYSIS AND RESULTS

Before presenting the results, we establish the notation to be used. As in [5], we characterize a template with N branches by means of two matrices: one of them is an $N \times N$ matrix called T in which T_{ii} is the number of half-turns of branch i $(i=0,1,2,\ldots)$ and T_{ij} $(i \neq j)$ is twice the linking number of the period-1 orbits embedded in branches i and j; the other one is a $1 \times N$ array I whose element I_j expresses the order of branch j within the pile formed by the whole set of branches when they converge into a single trunk (the higher the I_j, the higher the branch j appears in the pile). On the other hand, a period-m UPO which consecutively visits branches $i_1, i_2, \ldots, i_m$ will be referred to as $\overline{i_1 i_2 \ldots i_m}$. As usually, certainly all cyclic permutations of these symbols are different names for the same orbit, but they denote different intersection points between the UPO and a given PS (so, for instance, the orbit $\overline{i_1 i_2}$ intersects any PS at two points: the one called $\overline{i_1 i_2}$ is placed in the region i_1 of the generating partition and the one called $\overline{i_2 i_1}$ belongs to region i_2).

We have analyzed the emission of an erbium-doped ring laser with sine-wave modulated pump power. By choosing appropriate working conditions (average pump power, modulation depth, and modulation frequency), the laser emission shows chaotic behavior [23,24]. Several series $x(t_i)$ in different working conditions corresponding to chaotic behavior have been measured. The time series spread around 10^4 modulation periods, with 80–100 samples per period. A usual embedding for periodically driven systems was employed: $[x(t_i), x(t_i+\tau), \phi(t_i)]$, $\phi(t_i)$ being the sine-wave modulation phase at the time instant t_i and τ being around 5% of the pump modulation period. For each time series, various PSs for different fixed modulation phase values were drawn. The choice of τ allows us to obtain PSs without self-intersections (which appear if τ is too big; in some of our time series, self-intersections in the PSs were observed with τ around 10%) and not squeezed to the $x(t_i+\tau)=x(t_i)$ line (an effect appearing if τ is too small which makes the PS useless, as no

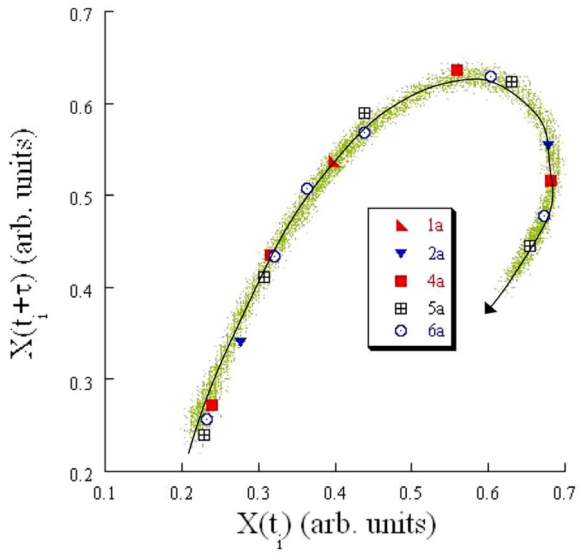

FIG. 1. (Color online) Poincaré section for pump modulation frequency $f=3.55$ kHz, modulation index $m=0.72$, and average pump power of 44 mW (pump wavelength: 1480 nm). The different dots represent intersections of different UPOs with the Poincaré section.

structure can be appreciated in it). On the other hand, a test based on principal component analysis corroborates that three dimensions suffice to describe this dynamical system correctly.

In the analysis of the series presented here we take profit of dealing with a highly dissipative system. In such situation, when representing its corresponding attractor in phase space one may expect to obtain PSs equivalent to a section of the template trunk, usually referred to as "branch line." A continuous parametrization all along this one-dimensional object can be defined, so that the first-return map with regard to the parameter chosen is an application. Besides, the kneading theory fixes the order of the semiflow intersections with the branch line and particularly the order of the UPO intersections. Therefore, a PS whose cloud of points is (approximately) distributed along a line is a candidate to constitute a good counterpart of the template branch line. In order to decide whether this PS is finally a good approximation of the branch line, a parametrization is defined and the first-return map with regard to the parameter chosen is drawn. Typically, the first-return map consists of a cloud of points distributed along a "relatively thick line" (the more dissipative the system, the thinner the line; a strictly one-dimensional plot would only be obtained in the limit of infinite dissipation). If the first-return plot obtained is one to one (save for the thickness of the cloud of points obtained), the PS can be considered a good representative of the branch line. Furthermore, the order of the UPOs marks both in the PS and in the first-return map must match the order fixed by the kneading theory.

Depending on our laser's working conditions, up to the moment we have found horseshoe, reverse horseshoe, and spiral templates. For the reasons previously commented, we consider the latter two as especially interesting, so we focus this work on the presentation of one example of each.

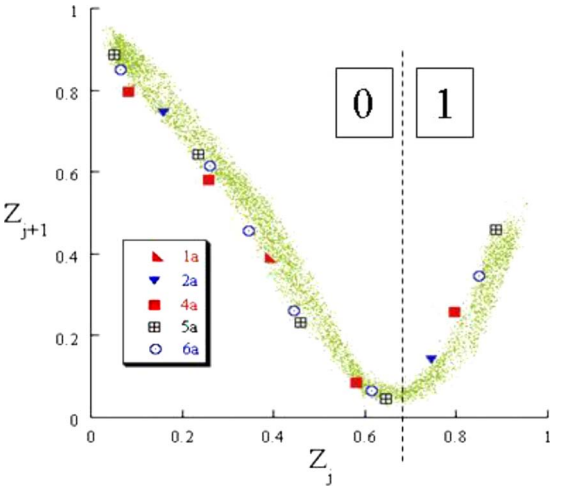

FIG. 2. (Color online) First return map as a function of the Z parameter obtained from the Poincaré section of Fig. 1. The different dots represent the Z parameters corresponding to the UPO intersections.

A. Reverse horseshoe

Figure 1 shows a PS in which the intersections of some of the UPOs found are pointed out (for the sake of clarity, we consider convenient not to show the intersections of all the UPOs found). The PS clearly meets the requirement of being approximately arranged along the line sketched in the plot (called L from now on). We define the coordinate Z of any point P belonging to L as the distance from the L tail to P along L, normalized so that $Z=1$ for the L head. For any point Q of the PS, we define its Z coordinate as the one of the point belonging to L closest to Q. Figure 2 shows the first-return map with regard to the Z coordinate. The cloud of points obtained appears arranged along a line corresponding to a one-to-one map. According to it, two regions [labeled 0 and 1] are enough to get a generating partition. The precise borderline between these regions is not perfectly defined. It could be achieved by means of the method shown in [25], but it is not necessary in this work: all the UPO intersections shown are far enough from the minimum, so that the region to which each one belongs is obvious. Therefore, the orbit names can be easily established: $1a=\overline{0}$, $2a=\overline{10}$, $4a=\overline{1000}$, $5a=\overline{10000}$, and $6a=\overline{100000}$.

On the other hand, the linking numbers of the UPOs detected were computed (Table I). The only template with two branches compatible with Table I is given by the following T and I matrices:

TABLE I. Linking numbers between the UPOs found in the time series corresponding to Fig. 1.

	$\overline{0}$	$\overline{10}$	$\overline{1000}$	$\overline{10000}$	$\overline{100000}$
$\overline{0}$	0				
$\overline{10}$	11	11			
$\overline{1000}$	22	45	67		
$\overline{10000}$	28	56	112	112	
$\overline{100000}$	33	67	134	168	167

TABLE II. Left: order of the intersections of orbits $\overline{0}$, $\overline{10}$, $\overline{100}$, $\overline{10000}$, and $\overline{100000}$ with the branching line, according to the kneading theory [considering template (2)]. Right: Z parameter obtained for intersections of orbits $1a$, $2a$, $4a$, $5a$, and $6a$ with the PS according to Fig. 1.

Symbolic sequence	Z parameter
$\overline{01000}$	0.051
$\overline{010000}$	0.065
$\overline{0100}$	0.082
$\overline{01}$	0.159
$\overline{00010}$	0.234
$\overline{000100}$	0.260
$\overline{0001}$	0.260
$\overline{000001}$	0.345
$\overline{0}$	0.389
$\overline{000010}$	0.444
$\overline{00001}$	0.460
$\overline{0010}$	0.582
$\overline{001000}$	0.614
$\overline{00100}$	0.644
$\overline{10}$	0.745
$\overline{1000}$	0.796
$\overline{100000}$	0.849
$\overline{10000}$	0.886

$$T=\begin{pmatrix}11 & 12\\ 12 & 12\end{pmatrix}=\begin{pmatrix}1 & 2\\ 2 & 2\end{pmatrix}+5\times\begin{pmatrix}2 & 2\\ 2 & 2\end{pmatrix},\quad I=(1\ \ 0),\quad (2)$$

that is, to say, a reverse horseshoe with an additional global torsion of five turns.

Note that some linking numbers shown in Table I are not possible if the underlying template is a Smale horseshoe: for instance, a linking number is equal to 45 between a period 2 and a period 4 UPO. Therefore, this result suffices to make sure that the system dynamics is organized according to a template different to the standard Smale horseshoe.

Finally, as an additional evidence of the correctness of the method employed, it is worthwhile to observe that the points corresponding to the UPOs follow the order fixed by the kneading theory both in the PS [Fig. 1(a)] and in the first-return map [Fig. 1(b)]. In order to facilitate the comparison, Table II provides the order of the different UPO intersections according to the kneading theory and their corresponding Z coordinates. The coincidence between kneading theory and Fig. 1 goes still further: there is a correlation between the distances between the UPO marks in Fig. 1 and the number of common symbols at the beginning of their respective symbolic chains. For instance, it is not surprising that the UPO marks corresponding to $\overline{00010}$, $\overline{000100}$, and $\overline{0001}$ appear close together, as they have seven common symbols at the beginning of their symbolic names. The same can be said about $\overline{000010}$ and $\overline{00001}$, which start with the same nine symbols.

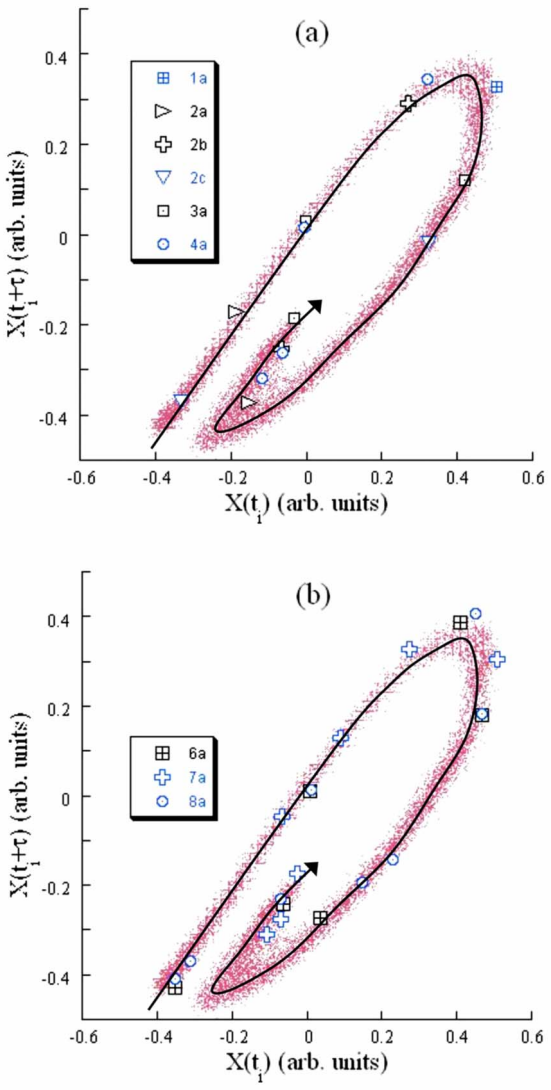

FIG. 3. (Color online) Poincaré section for pump modulation frequency $f=3.65$ kHz, modulation index $m=0.70$, and average pump power of 38 mW (pump wavelength: 1480 nm). Intersections of the lowest period UPOs with the Poincaré section are shown in (a) and intersections of other UPOs are pointed out in (b).

B. Spiral template

The procedure summarized above has also been applied to the PS shown in Fig. 3. For the sake of clarity, only the lowest period UPOs found have been represented in Fig. 3(a), while some other UPOs significant in the analysis (as explained next) are shown in Fig. 3(b). The first-return map obtained is shown in Fig. 4. In this case, the map presents a maximum and a minimum which means that there are three regions in the generating partition, labeled as 0, 1, and 2. Again, the borderlines between these regions cannot be established precisely, especially the one between regions 1 and 2, corresponding to a considerably smoothed minimum; that is why we separate regions 1 and 2 by means of a shaded "area of uncertainty." However, there is no doubt about the symbolic names corresponding to most of the UPOs shown: $1a=\overline{1}$, $2a=\overline{20}$, $2b=\overline{21}$, $2c=\overline{10}$, $3a=\overline{210}$, $4a=\overline{2120}$,

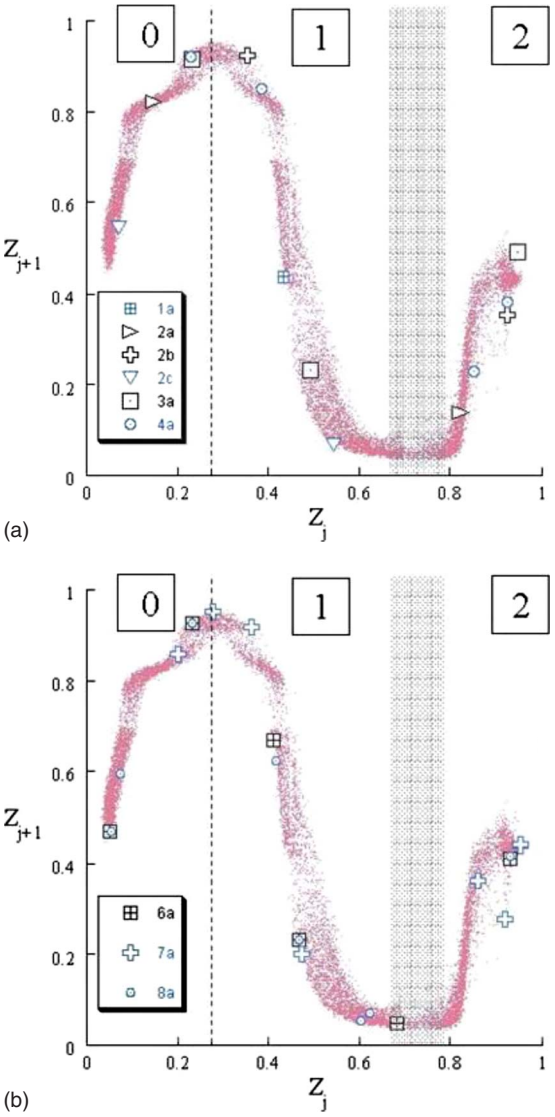

FIG. 4. (Color online) First return map as a function of the Z parameter obtained from the Poincaré section of Fig. 3. The different dots in (a) and (b) represent the Z parameters corresponding to the UPO intersections shown in Figs. 3(a) and 3(b), respectively.

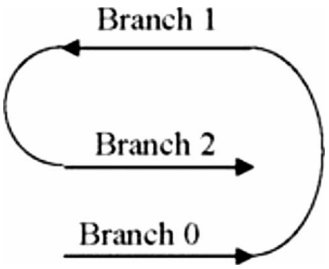

FIG. 5. Folding mechanism of an outside-to-inside spiral template with three branches.

and $8a=\overline{10101021}$. Concerning UPO $7a$, one of its marks appears in the maximum of the first-return map, so we consider two possible symbolic names: $\overline{1202102}$ and $\overline{1212102}$. On the other hand, one of the marks of the UPO $6a$ appears in the shaded area. Therefore, two symbolic names are possible: $\overline{101021}$ and $\overline{201021}$.

Table III shows the linking numbers between each pair of these UPOs, save for the cases in which there was uncertainty in its determination due to noise in the experimental time signal. The only template compatible with the linking numbers found and the established UPO symbolic names is

$$T=\begin{pmatrix}8&8&8\\8&9&10\\8&10&10\end{pmatrix}=\begin{pmatrix}0&0&0\\0&1&2\\0&2&2\end{pmatrix}+4\times\begin{pmatrix}2&2&2\\2&2&2\\2&2&2\end{pmatrix},$$

$$I=(0\ \ 2\ \ 1), \tag{3}$$

that is to say, an outside-to-inside spiral [8] with a global torsion of four turns, whose folding mechanisms are summarized in Fig. 5. It must be cleared up that template (3) is the only compatible template no matter which ones of couples of possible symbolic names for orbits $6a$ and $7a$ are considered. On the other hand, it is worthwhile to underline that only two linking numbers (LKs) in Table III allow us to make the difference between the template found and an inside-to-outside spiral [8]: it deals with LK$(6a,7a)$ and LK$(7a,\overline{10101021})$.

TABLE III. Linking numbers between the UPOs found in the time series corresponding to Figs. 3 and 4. Asterisks appear instead of the linking numbers whose determination has been impossible due to the noise in the experimental time signal.

	$\overline{1}$	$\overline{20}$	$\overline{21}$	$\overline{10}$	$\overline{210}$	$\overline{2120}$	$6a$	$7a$	$\overline{10101021}$
$\overline{1}$	0								
$\overline{20}$	9	9							
$\overline{21}$	9	18	9						
$\overline{10}$	9	18	18	9					
$\overline{210}$	14	27	28	27	28				
$\overline{2120}$	18	*	*	36	55	55			
$6a$	27	54	55	*	*	109	135		
$7a$	32	63	65	63	97	*	191	194	
$\overline{10101021}$	36	72	73	*	*	145	*	254	251

Furthermore, as in the reverse horseshoe case, the order of the UPO intersections predicted by the kneading theory agrees with the one observed both in Figs. 3 and 4 (in this case a table similar to Table II seems to us too lengthy to be included here). Besides, UPO intersections which appear especially close correspond to pairs of symbolic sequences whose beginnings share several common symbols: $\overline{021}$ and $\overline{0212}$ almost overlap; likewise $\overline{21}$ and $\overline{2120}$; and especially, orbits 6*a* and 8*a* overlap four times, not surprisingly because they share a common sequence of at least five symbols: 01021.

IV. CONCLUSIONS

Two chaotic time series obtained from the emission of an erbium-doped fiber laser with appropriate sine-wave pump modulation conditions have been analyzed. It has been found that the corresponding chaotic attractors present topological structures not often observed in experimental systems: the reverse horseshoe and the spiral template. These results, different from the Smale horseshoe commonly obtained in other experimental studies, contribute to enforce the relevance of topological procedures of characterization aimed at the template determination.

Furthermore, application of an especially simple method of analysis has been possible, thanks to dealing with a highly dissipative system. This feature allows one to find PSs which constitute good approximations of the template branch line. By a suitable parametrization all along these PSs, one-to-one first-return maps with regard to the parameter chosen are obtained which lead to the determination of a generating partition precise enough to assign symbolic names to most of the different UPOs found. This property simplifies the procedure of analysis dramatically with regard to the usual situation in which a generating partition is not available beforehand. Besides, it allows one to check the consistency of the results obtained by comparing the order of the UPO intersections found with the order fixed by the kneading theory.

ACKNOWLEDGMENT

This work was supported by the CICYT under Project No. FIS2006-03649.

[1] J. S. Birman and R. F. Williams, Topology **22**, 47 (1983).
[2] J. S. Birman and R. F. Williams, Contemp. Math. **20**, 1 (1983).
[3] R. W. Ghrist, P. J. Holmes, and M. C. Sullivan, *Knots And Links In Three-Dimensional Flows*, Lecture Notes in Mathematics Vol. 1564 (Springer, Berlin, 1997).
[4] M. A. Natiello and H. G. Solari, *The User's Approach To Topological Methods In 3D Dynamical Systems* (World Scientific, Singapore, 2007).
[5] G. B. Mindlin, X. J. Hou, H. G. Solari, R. Gilmore, and N. B. Tufillaro, Phys. Rev. Lett. **64**, 2350 (1990).
[6] R. Gilmore, Rev. Mod. Phys. **70**, 1455 (1998).
[7] N. B. Tufillaro, T. Abbott, and J. Reilly, *An Experimental Approach to Nonlinear Dynamics and Chaos* (Addison Wesley, Reading, 1992).
[8] R. Gilmore and M. Lefranc, *The Topology of Chaos* (Wiley, New York, 2002).
[9] H. G. Solari, M. A. Natiello, and M. Vazquez, Phys. Rev. E **54**, 3185 (1996).
[10] A. Fioretti, F. Molesti, B. Zambon, E. Arimondo, and F. Papoff, Int. J. Bifurcation Chaos Appl. Sci. Eng. **3**, 559 (1993).
[11] L. Kocarev, Z. Tasev, and D. Dimovski, Phys. Lett. A **190**, 399 (1994).
[12] N. B. Tufillaro, P. Wyckoff, R. Brown, T. Schreiber, and T. Molteno, Phys. Rev. E **51**, 164 (1995).
[13] G. Boulant, S. Bielawski, D. Derozier, and M. Lefranc, Phys. Rev. E **55**, R3801 (1997).
[14] R. Gilmore, X. Pei, and F. Moss, Chaos **9**, 812 (1999).
[15] G. Boulant, Ph.D. thesis, University of Lille I, 1997.
[16] G. Boulant, M. Lefranc, S. Bielawski, and D. Derozier, Int. J. Bifurcation Chaos Appl. Sci. Eng. **8**, 965 (1998).
[17] C. Letellier, G. Gouesbet, and N. Rulkov, Int. J. Bifurcation Chaos Appl. Sci. Eng. **6**, 2531 (1996).
[18] G. Boulant, J. Plumecoq, S. Bielawski, D. Derozier, and M. Lefranc, *Proceedings of the Fourth Experimental Chaos Conference*, Boca Raton (World Scientific, Singapore, 1998), pp. 121–126.
[19] F. Papoff *et al.*, Phys. Rev. Lett. **68**, 1128 (1992).
[20] M. Lefranc *et al.*, Phys. Rev. Lett. **73**, 1364 (1994).
[21] P. So, E. Ott, S. J. Schiff, D. T. Kaplan, T. Sauer, and C. Grebogi, Phys. Rev. Lett. **76**, 4705 (1996).
[22] L. LeSceller, C. Letellier, and G. Gouesbet, Phys. Rev. E **49**, 4693 (1994).
[23] L. G. Luo, T. J. Tee, and P. L. Chu, J. Opt. Soc. Am. B **15**, 972 (1998).
[24] I. J. Sola, J. C. Martín, and J. M. Álvarez, Opt. Commun. **212**, 359 (2002).
[25] J. Plumecoq and M. Lefranc, Physica D **144**, 231 (2000).